Chapter 4

Intrinsic Microcrystalline Silicon

The relation between the structure properties, in particular the ratio between crystalline and amorphous volume content, and the electronic properties of the material is of great interest. Especially since it has been shown, that contrary to what one might expect, material prepared close to the transition to amorphous growth yields the highest solar cell conversion efficiencies, rather than material with the largest crystalline grain size and the highest crystalline volume fractions. In this Chapter, paramagnetic states found in intrinsic μc-Si:H are identified and correlated to the structure properties of the material. ESR measurements, on intrinsic μc-Si:H prepared by HWCVD under various deposition conditions leading to material with structure compositions varying from highly crystalline to fully amorphous are described. Additionally, data from a PECVD series prepared and studied by Baia Neto et al. [17, 18, 160] is reanalyzed and compared with results obtained for the HWCVD material.

4.1 Raman Spectroscopy

In Fig. 4.1 Raman spectra of μc-Si:H prepared on different substrates are shown. The silane concentration SC=[SiH_4]/([H_2]+[SiH_4]) was chosen to result in (a) highly crystalline material and (b) material at the transition between crystalline and amorphous growth. With increasing SC the amorphous phase content in the film increases, resulting in an increasing contribution of the amorphous signal in the Raman spectra around 480 cm^{-1}. While the highly crystalline material, shown in panel (a), shows no difference in the spectra of films prepared on glass or aluminum, the structure of the material prepared at the transition between crystalline and amorphous growth depends strongly on the substrate used (see panel (b)). Material deposited on glass substrates shows a much stronger contribution of the amorphous peak than that deposited on aluminum. This substrate dependence has

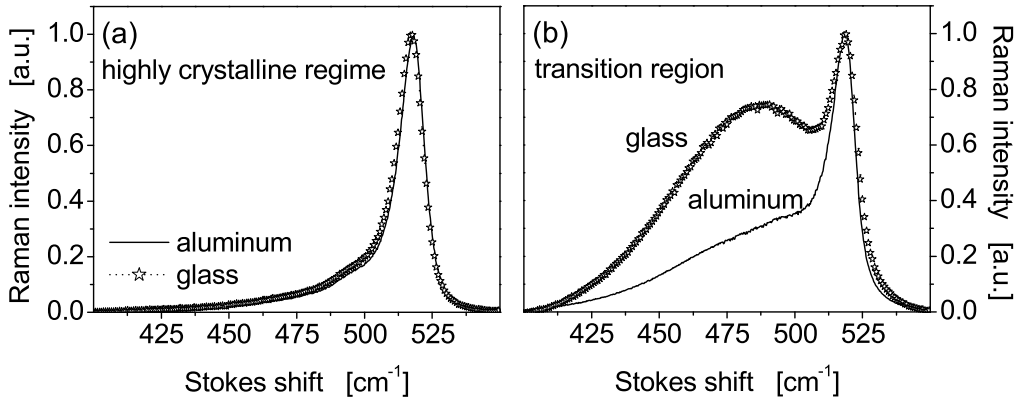

Figure 4.1: *Raman spectra of material prepared on different substrates under deposition conditions resulting (a) in highly crystalline material and (b) material at the transition between crystalline and amorphous growth.*

to be kept in mind, as in the following chapters conductivity measurements are compared with results obtained from ESR, for which glass and aluminum substrates have been used. In particular, a comparison of material properties near the transition between microcrystalline and amorphous growth has to be made carefully.

The structural properties of the deposited films are not determined solely by the silane concentration and the substrate. In Fig. 4.2 the Raman intensity ration I_C^{RS}, determined as described in section 3.1.1, is shown as a function of SC for a number of samples prepared with (a) PECVD (taken from reference [160]) and (b) HWCVD prepared at different substrate temperatures ranging from T_S = 185°C to T_S = 450°C. For all series, the silane concentration was varied covering the complete range from highly crystalline to predominately amorphous growth. Except for the HW material prepared at T_S = 450°C, for which glass substrates were used, all spectra were taken from material deposited on aluminum substrates. Independent of the particular deposition parameter or deposition process, one observes a decrease of I_C^{RS} with increasing SC. The qualitative behavior upon changes of SC are the same and is discussed for the VHF material, plotted in Fig. 4.2 (a). Between $SC = 2-4\%$, I_C^{RS} decreases only slightly, from 0.80 to 0.74, indicating a highly crystalline structure. Above $SC = 4\%$ an increasing amorphous phase content results in a decreasing I_C^{RS} and for silane concentrations higher than 7% only an amorphous phase contribution can be observed in the Raman signal. The region $SC = 4\%-7\%$ is referred to as the transition zone. Within this regime of deposition parameters, the material structure changes from crystalline to predominately amorphous. The position and width of the zone strongly depends on the deposition parameters used, e.g. the substrate temperature during

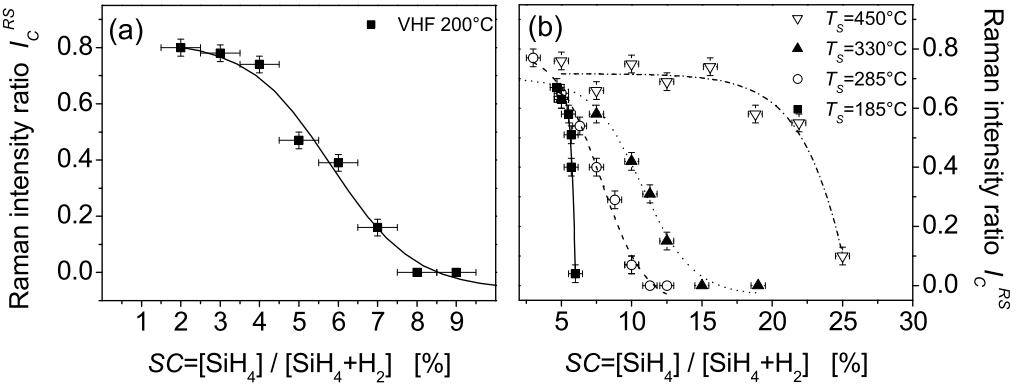

Figure 4.2: *Raman intensity ratio of (a) VHF-PECVD material and (b) HWCVD-material deposited at different substrate temperatures ranging from T_S = 185°C to T_S = 450°C taken from reference [17, 18, 160] and [13], respectively.*

the process plays an important role for the structural development of the films. This is shown in Fig. 4.2 (b), where the I_C^{RS} of HW-material prepared at different T_S is shown. An increasing T_S leads to a shift of the transition to higher values of SC. The dependency on T_S has been also observed for PECVD material [161].

The observed shifts of the transition under different deposition conditions make it difficult to use the silane concentration as a single parameter to predict the electronic properties of samples prepared under different conditions. Even material prepared in the same run, but on different substrates, may show different properties. Therefore, in the following sections the Raman intensity ratio I_C^{RS}, rather than SC, will be used to compare electronic properties of different samples.

4.2 Electrical Conductivity

Within this section, a short review of the conductivity data of both the PECVD and the HWCVD material taken from references [17] and [13], respectively, will be given. These results are of particular importance for the following Chapters and will therefore briefly be reviewed in this context.

The transition in growth is directly reflected in the conductivity as shown in Fig. 4.3. Here, results of dark conductivity σ_D measurements are plotted versus the Raman intensity ratio I_C^{RS} for material prepared using (a) VHF-PECVD and (b) HWCVD. Plotting σ_d versus I_C^{RS} has recently become a widely used method to compare material prepared under different deposition conditions and in different systems (see e.g. [16, 13]). All samples show the same general depen-

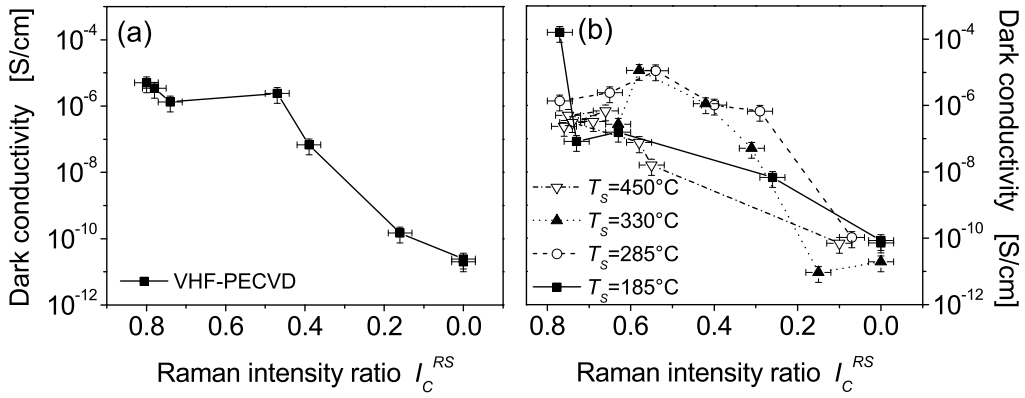

Figure 4.3: *Dark conductivity σ_D as a function of I_C^{RS} of material prepared with (a) VHF-PECVD and (b) HWCVD at various substrate temperatures, taken from reference [17, 18] and [13], respectively.*

dency of σ_D upon I_C^{RS}. Material prepared in the crystalline growth regime shows a dark conductivity of 10^{-4} to 10^{-7} S/cm, which is of the same order of magnitude as observed for crystalline silicon. However, in c-Si the electron mobilities ($\mu \approx 1500$ cm^2/Vs [91]) exceed by far the electron mobilities in μc-Si:H (a few cm^2/Vs [49]). This suggests a considerable background doping in intentionally undoped μc-Si:H. As a consequence of the structural transition, for material with an I_C^{RS} lower than 0.4 σ_D decreases by several orders of magnitude, resulting in values below 10^{-10} S/cm, which is typical for a-Si:H [65]. When comparing material prepared in the transition regime, the drop in σ_D occurs at slightly higher values of I_C^{RS} for the material prepared with PECVD compared to that prepared with HWCVD. For material prepared with HWCVD one observes subsequent lower values of the conductivity for substrate temperatures of $T_S = 450$°C and 185°C. Anticipating results obtained in the next section, the low σ_D of the $T_S = 450$°C material can be explained by a high defect density. On the other hand, the $T_S = 185$°C material shows very low spin density. The low values of σ_D might therefore be a result of a reduced impurity level or reduced mobility caused by grain boundary effects.

4.3 ESR Signals and Paramagnetic States in Intrinsic μc-Si:H

ESR measurements were performed on powdered material deposited on aluminum substrates. Details of the powder preparation process can be found in section 3.3.1.

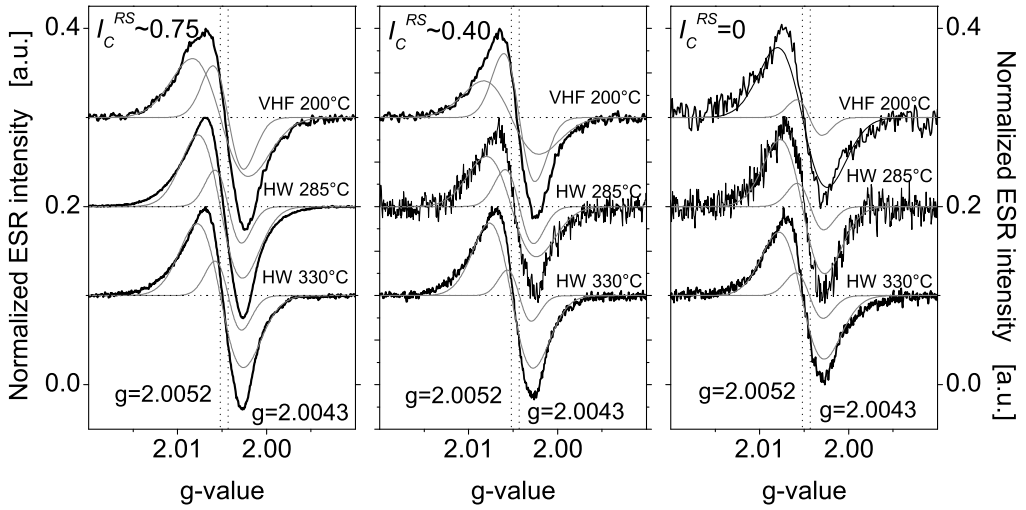

Figure 4.4: *Typical ESR spectra of VHF-PECVD and HWCVD material with structure compositions varying from highly crystalline ($I_C^{RS} \approx 0.75$) to fully amorphous ($I_C^{RS} \approx 0$). The discrepancy for the crystalline HW-material is a result of post-oxidation of these highly porous structures. A detailed study of these effects can be found in Chapter 6.*

Fig. 4.4 shows typical ESR spectra taken on material with different crystallinity prepared with VHF-PECVD and HWCVD. The structure varies from highly crystalline ($I_C^{RS} \approx 0.75$) to material at the transition between crystalline and amorphous growth ($I_C^{RS} \approx 0.4$) and finally to material which shows no contribution of the crystalline phase in the Raman spectra ($I_C^{RS} = 0$). All spectra show the typical asymmetric line shape with contributions at g=2.0043 and g=2.0052, in the following denoted as db_1 and db_2, respectively. Numerical fits to the measured data are included in the graphs, as gray lines. Interestingly, the line width of the two resonances changes only little upon different structure compositions and the width is also similar for material prepared with either PECVD or HWCVD. Optimum fits of the superimposed lines could be performed using Gaussian lines with line widths of $\Delta H_{pp} = 5.6 \pm 0.3$ G for the db_1 and $\Delta H_{pp} = 9.7 \pm 0.5$ G for the db_2 resonance. However, while these fits work perfectly for the PECVD material, some deviations can be observed for the HWCVD material. In particular, at the high g-value site of the spectra, the two resonances does not fit the spectra correctly. This is a result of post-oxidation of these highly porous structures and will be extensively studied in Chapter 6.

Looking at the VHF-PECVD material (uppermost spectra), one observes that for the highly crystalline material the spectrum is dominated by the db_2 resonance, while for material prepared at the μc-Si:H/a-Si:H transition with $I_C^{RS} \approx 0.40$ the resonance at g=2.0043 contributes much more to the overall ESR signal, resulting

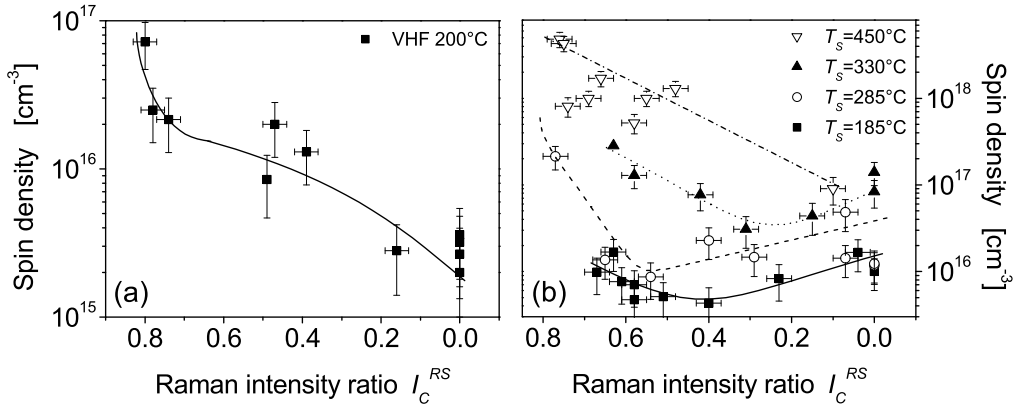

Figure 4.5: *Spin density as a function of I_C^{RS} for μc-Si:H prepared with (a) VHF-PECVD and (b) HWCVD deposited at various substrate temperatures. The values for the VHF-PECVD material were taken from reference [17].*

in a shift of the average g-value[1] with respect to lower values. For material with no discernable crystalline signal in the Raman spectra ($I_C^{RS} = 0$, right panel), the g-value shifts to higher values, however, without reaching the value of g=2.0055 characteristically observed in a-Si:H. The signal is clearly dominated by the resonance at g=2.0052. The same trend can be also observed for the HW material prepared at $T_S = 285$°C (see Fig. 4.4). For the highly crystalline and amorphous material the spectra are dominated by the db_2 resonance at g=2.0052, while for the material at the μc-Si:H/a-Si:H transition an increasing contribution of the db_1 line can be observed. Material prepared at substrate temperatures as high as $T_S = 330$°C, regardless of the structure composition all spectra are dominated by the db_2 resonance. It is important to note, that for a fixed I_C^{RS} the increasing contribution of the db_2 resonance goes along with an increasing overall spin density N_S. This issue will be discussed in more detail below.

The spin density N_S obtained from numerical integration of the ESR spectra is plotted in Fig. 4.5 versus the Raman crystallinity I_C^{RS}. Remarkably, independent of the deposition technique and deposition conditions used, the highest spin densities are always observed for the material with the highest crystallinity. For the VHF-PECVD material, plotted in Fig. 4.5 (a), N_S decreases slightly between $I_C^{RS} = 0.78$ and 0.39. At the highest crystallinity, N_S increases steeply from 2.5×10^{16} cm^{-3} at $I_C^{RS} = 0.78$ to values of 7.2×10^{16} cm^{-3} at $I_C^{RS} = 0.80$. Beyond the transition to amorphous growth ($I_C^{RS} < 0.39$), the spin density drops further down by one order of magnitude to values as low as 2×10^{15} cm^{-3}.

[1]The average g-value is defined as the zero-crossing of the ESR signal.

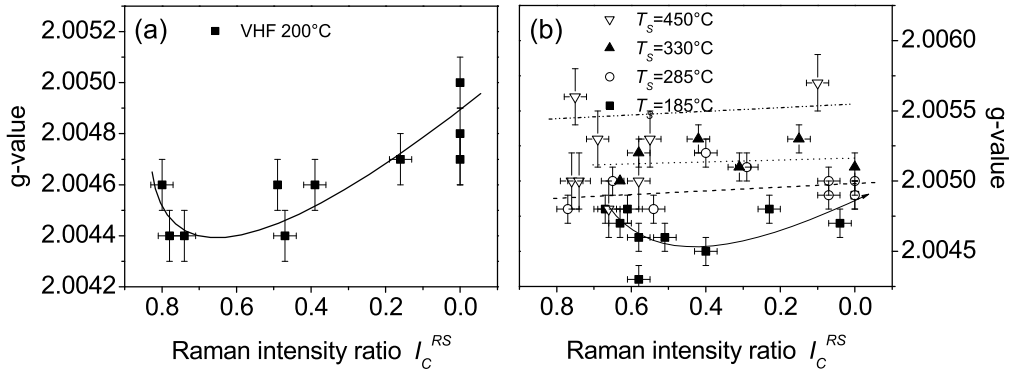

Figure 4.6: *g-values as a function of I_C^{RS} of material prepared (a) VHF-PECVD and (b) HWCVD deposited at various substrate temperatures. The values for the VHF-PECVD material were taken from reference [17].*

For the HWCVD material, again the highest N_S is always found for material with the highest crystallinity. Within the crystalline regime, the spin density decreases considerably with increasing amorphous content for all substrate temperatures T_S. For material dominated by amorphous phase content ($I_C^{RS} < 0.4$), the spin density increases, rather than staying constant or decreasing as observed for the PECVD material. Only for the highest T_S of 450°C the spin density decreases monotonously, however at very high values of $N_S > 10^{17}$ cm^{-3}. Finally, independent of the particular structure composition, N_S increases significantly when the substrate temperature is increased by up to three orders of magnitude for $I_C^{RS} \approx 0.5$. It is important to note that the lowest spin densities of $N_S = 4 \times 10^{15}$ cm^{-3} are observed for material prepared at $T_S = 185$°C and a crystalline volume fraction of $I_C^{RS} \approx 0.4$, and that solar cells prepared under similar conditions have shown maximum efficiencies of $\eta = 9.4\%$ [162].

The corresponding average g-values are plotted versus I_C^{RS} in Fig. 4.6. For the PECVD material shown in Fig. 4.6 (a), the average g-value shifts from a value of 2.0043 to 2.0051, when going from crystalline to amorphous structure. This means that with increasing amorphous content the g-value is clearly shifted to higher values, however without reaching the value of 2.0055 usually found in a-Si:H. As shown in Fig. 4.6 (b), the g-values for material prepared with HWCVD are generally higher (note the different scaling of the y-axis in panels (a) and (b)). The variations as a function of structure are considerably less for the HW-material. Again, even for material with no contribution of the crystalline phase in the Raman signal, the g-values do not reach the typical value of 2.0055 found in a-Si:H. Generally, one observes an increasing g-value for increasing substrate temperature over the entire range of I_C^{RS}.

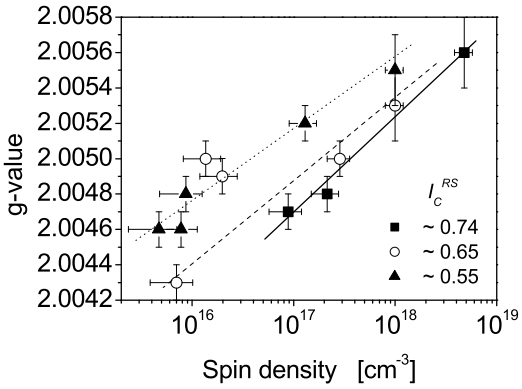

Figure 4.7: *g-value vs. spin density N_S of material prepared with HWCVD for three structure compositions ranging from highly crystalline to transition material. The data are taken from Fig. 4.5 (b) and 4.6 (b).*

Comparing Fig. 4.5 (b) and Fig. 4.6 (b), one can observe that both N_S and the g-value increase with increasing substrate temperature T_S. In Fig. 4.7 the g-value is plotted versus N_S for three different structure compositions, ranging from highly crystalline to material prepared close to the transition between microcrystalline and amorphous growth. The values of N_S and g were taken from Fig. 4.5 and 4.6, respectively; the data points in Fig. 4.8 therefore correspond to material prepared at different substrate temperatures. Although there is some scatter of the data for the $I_C^{RS} \approx 0.65$ material, there is a clear correlation between this two quantities: For increasing spin density the g-value is clearly shifted to higher values. This can be observed for all structure compositions between $I_C^{RS} = 0.74$ and 0.55. Assuming that within the crystalline regime the ESR signal is a composition of only two resonances at g=2.0043 and g=2.0052, the shift of the average g-value is a result of a change in the ratio of these contributions. This of course also assumes that the g-value of each line does not shift for different deposition conditions, which is a rather strong postulation. Keeping this in mind, the results indicate that the increasing spin density N_S, as a function of increasing T_S, is caused by an increasing number of paramagnetic states that belong to the db_2 resonance.

The fact that high quality μc-Si:H material with no discernable crystalline signal in the Raman signal does not show the typical a-Si:H g-value of 2.0055 was a little puzzling. Material has therefore been prepared with even higher silane concentrations ranging from $SC = 9\%$ to 100% using VHF-PECVD. Spin densities and g-values measured for this material are plotted in Fig. 4.8 along with the

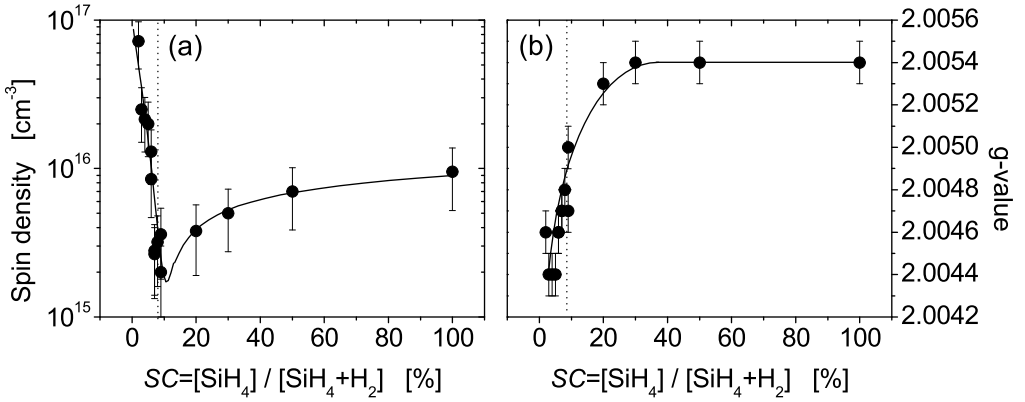

Figure 4.8: *(a) Spin density and (b) g-value of material prepared by VHF-PECVD varying the silane concentration in the range between $SC = 2 - 100\%$.*

values previously plotted in Fig. 4.5 (a) and Fig. 4.6 (a). The dotted vertical line indicates the threshold to fully amorphous growth. For SC higher than this value, the Raman spectra show no contribution of the crystalline signal on both, material prepared on aluminum and glass substrates. As shown before, the spin density decreases monotonously between $SC = 2$ and 9% from $N_S = 7.2 \times 10^{16}$ cm^{-3} to very low values of $N_S = 2 \times 10^{15}$ cm^{-3}. With increasing silane concentration N_S increases again reaching a value of 1×10^{16} cm^{-3} for a source gas mixture containing only SiH_4, which is a typical value for high quality amorphous silicon [65]. Far more interesting is the development of the g-value shown in Fig. 4.8 (b). Right beyond the transition, although no contribution of a crystalline signal can be observed in the Raman spectra, the g-value is still at low values of g=2.0050. A further increased silane concentration then leads to a shift of the g-value towards g=2.0054 typically observed for a-Si:H.

4.4 Discussion - Relation between ESR- and Structural Properties

Independent of the particular deposition process, VHF-PECVD or HWCVD, the ESR signal of intrinsic μc-Si:H shows an asymmetric line, which could be well fitted by two Gaussian contributions, db_1 and db_2, at g=2.0043 and g=2.0052 with line widths of $\Delta H_{pp} = 5.6 \pm 0.3$ and $\Delta H_{pp} = 9.7 \pm 0.5$ G, respectively. For structure compositions of the full range, from highly crystalline to fully amorphous, the highest spin densities N_S are always observed for material with the highest crystallinity, while an increasing amorphous content leads to a decreasing num-

ber of paramagnetic states. This also applies for the substrate temperature T_S, where an increasing T_S results in an increasing N_S. Interestingly, an increasing spin density also leads to a shift of the average g-value with respect to higher values, as has been shown in Fig. 4.6. As the ESR signal of μc-Si:H generally can be deconvoluted into two contributions db_1 and db_2, it is tempting to relate the shift of the average g-value to variations of the intensity ratio of these two signals. Whereas the ESR spectra of highly crystalline, but well passivated material is dominated by the db_1 resonance, additional defects result in the db_2 resonance at g=2.0052 (compare also Fig. 4.4). On the other hand, an increasing amorphous phase content leads to a higher contribution of the db_2 resonance to the overall signal. Interestingly, the peak to peak line width ΔH_{pp} of the individual signals (db_1, db_2) changes only little upon variations of the defect density or the structure composition. If the line width is dominated by inhomogeneous broadening, i.e. disorder effects, this suggests little variation of the local disorder surrounding the DB-defects, for the various samples investigated.

There is still no conclusive evidence on what is the origin of the resonances db_1 (g=2.0043) and db_2 (g=2.0052), typically found in μc-Si:H. The particular structure of μc-Si:H allows for a number of places where dangling bond defects are possibly located: the crystalline regions; the grain boundaries; the amorphous phase or in connection with impurity atoms, e.g. oxygen. However, some conclusions can be drawn from these results. Assuming that the two resonances are the result of two independent states, which is not yet proven, the contribution of db_2 resonance increases upon increasing T_S and amorphous phase content. Over this wide range of samples, the line width ΔH_{pp} remains fairly constant at values of $\Delta H_{pp} = 9.7 \pm 0.5$ G, which is close to the value of $\Delta H_{pp} \approx 10$ G found in a-Si:H [85]. However, because of the two facts that (i) the overall N_S strongly decreases with increasing amorphous content and (ii) poor passivated highly crystalline material with no amorphous phase content is also dominated by the resonance at g=2.0052, it seems unlikely that the amorphous phase itself is the origin of the paramagnetic states. More likely, the defects are located at grain boundaries, whether on the crystalline grains forming the columnar structures or at the outside of the columns. From X-ray analysis one derives typical sizes of the crystalline grains between $4-20$ nm [58]. Assuming an average size of a coherent region of 12 nm edge length, cubic grains, and a sample average spin density of $N_S = 2\times10^{16}$ cm^{-3}, there is only one defect per 30 grains. This is in agreement with the fact that the small crystalline grains are separated from each other by twin boundaries and stacking faults, which are known to preserve the local tetrahedral coordination and are not expected to lead to paramagnetic defects. It seems therefore more likely that the defects are located at the boundaries of the columnar clusters, as has been suggested before [161].

This is supported by the ESR data obtained for different substrate tempera-

tures. As observed in Fig. 4.5 (b), N_S increases as a function of T_S, independent of the structure composition. Infrared studies have shown that with increasing T_S, the amount of hydrogen incorporated in the material decreases significantly [13], which can be ascribed to an aggravated desorption of hydrogen during the growth process. The increasing N_S, which is accompanied by a shift of g to higher values, indicates that the increasing spin density is associated with an increasing number of db_2 states. Because the bonded hydrogen is located mainly at the column boundaries, which passivates dangling bonds, one can conclude that the desorption leads to un-terminated db_2 states residing at the column boundaries.

The question whether the ESR signal for both materials, prepared at high T_S or high amorphous phase content, is a result of the same paramagnetic states cannot be decided. In this context it is interesting that even fully amorphous material prepared at the microcrystalline/amorphous transition shows the resonance at g=2.0052, rather than the expected value of g=2.0055. Also, the observed line width of the db_2 resonance is essentially the same as observed in the highly crystalline regime. The differences of the g-value, compared to that observed in a-Si:H might be a result of a different medium range order in this so-called "polymorphous", "protocrystalline", or "edge-material" [163]. Speculatively, one might conclude that the degree of disorder around the defects is comparable to that found around the paramagnetic states located at the column boundaries. To answer this question remains a challenge for future investigations.

Similarly to a-Si:H, in the microcrystalline regime ($I_C^{RS} = 0.85 - 0.4$), the observed spin density correlates nicely with the energy conversion efficiency of the solar cells, containing the same absorber layer. Independent of the particular deposition process, it was found that not, as one might have expected, material with the highest crystalline volume fractions, but material prepared close to the transition to amorphous growth yields the highest solar cell conversion efficiencies. The performance of the solar cell increases slightly with increasing amorphous content from $I_C^{RS} = 0.71 - 0.5$. On the other hand, material with the highest crystalline volume fraction leads to very poor conversion efficiencies. Apparently, the highest crystallinity and the largest grain size is only obtained at the cost of a poor defect passivation. By contrast, the increasing amorphous phase content incorporated between the crystalline columns, is a highly efficient passivation layer and the increasing hydrogen content leads to a better termination of surface states. A critical relation between N_S and solar cell performance is also found for the variation of the substrate temperature. Again, material which shows the highest solar cell conversion efficiency is found to have the lowest spin density. It is likely, that the optimum of T_S is because of this hydrogen desorption problem, just as for a-Si:H deposition.

4.5 Summary

In the previous section, the results of the study on paramagnetic defects in undoped μc-Si:H were presented. For structure compositions ranging from highly crystalline to fully amorphous, the highest N_S is always found for material with the highest I_C^{RS}. While the preparation within this regime leads to the highest crystallinity and the largest grain sizes, this can be achieved only at the cost of a poor defect passivation. The increasing SC during the process leads to a better termination of the surface states caused by the increasing hydrogen content. On the other hand, additional amorphous phase content, incorporated between the crystalline columns, acts as a passivation layer and leads to a better termination of surface states. Very low N_S are found for material close to or beyond the transition to amorphous growth (see Fig. 4.5 (a)). For HWCVD material a strong dependence of the spin density N_S on the deposition temperature T_S was found. Generally, the increasing spin density, caused by either low SC or high T_S during the deposition process leads to an increasing contribution of the db_2 resonance. On the other hand, the g-value shifts to higher values with increasing amorphous content. Surprisingly, even material prepared close to the structural transition, with no discernable crystalline signal in the Raman spectra, does not show the typical a-Si:H value of g=2.0055. In fact, the ESR signal is clearly dominated by the resonance at g=2.0052. Only for material prepared at yet higher silane concentrations can g=2.0055 be detected (see Fig. 4.8). Whether the differences of the g-value compared to that observed in a-Si:H are the result of a different medium range order [61] cannot be determined from these data and remains e a task for future investigation. A detailed study of material prepared at transition between microcrystalline and amorphous growth using TEM and ESR, could provide further information on how changes of the structure, in particular the medium range order, affect the position of the resonance line observed in ESR. This might also provide further details concerning the nature of defects in μc-Si:H.